2018

A silicon strip detector array for energy verification and quality assurance in heavy ion therapy

Emily Debrot
University of Wollongong, ed827@uowmail.edu.au

Matthew Newall
University of Wollongong, mkn282@uowmail.edu.au

Susanna Guatelli
University of Wollongong, susanna@uow.edu.au

Marco Petasecca
University of Wollongong, marcop@uow.edu.au

Naruhiro Matsufuji
National Institute Of Radiological Sciences, matufuji@nirs.go.jp

See next page for additional authors

A silicon strip detector array for energy verification and quality assurance in heavy ion therapy

Abstract

Purpose

The measurement of depth dose profiles for range and energy verification of heavy ion beams is an important aspect of quality assurance procedures for heavy ion therapy facilities. The steep dose gradients in the Bragg peak region of these profiles require the use of detectors with high spatial resolution. The aim of this work is to characterize a one dimensional monolithic silicon detector array called the “serial Dose Magnifying Glass” (sDMG) as an independent ion beam energy and range verification system used for quality assurance conducted for ion beams used in heavy ion therapy.

Methods

The sDMG detector consists of two linear arrays of 128 silicon sensitive volumes each with an effective size of 2mm × 50μm × 100μm fabricated on a p-type substrate at a pitch of 200 μm along a single axis of detection. The detector was characterized for beam energy and range verification by measuring the response of the detector when irradiated with a 290 MeV/u ^{12}C ion broad beam incident along the single axis of the detector embedded in a PMMA phantom. The energy of the ^{12}C ion beam incident on the detector and the residual energy of an ion beam incident on the phantom was determined from the measured Bragg peak position in the sDMG. Ad hoc Monte Carlo simulations of the experimental setup were also performed to give further insight into the detector response.

Results

The relative response profiles along the single axis measured with the sDMG detector were found to have good agreement between experiment and simulation with the position of the Bragg peak determined to fall within 0.2 mm or 1.1% of the range in the detector for the two cases. The energy of the beam incident on the detector was found to vary less than 1% between experiment and simulation. The beam energy incident on the phantom was determined to be (280.9 ± 0.8) MeV/u from the experimental and (280.9 ± 0.2) MeV/u from the simulated profiles. These values coincide with the expected energy of 281 MeV/u.

Conclusions

The sDMG detector response was studied experimentally and characterized using a Monte Carlo simulation. The sDMG detector was found to accurately determine the ^{12}C beam energy and is suited for fast energy and range verification quality assurance. It is proposed that the sDMG is also applicable for verification of treatment planning systems that rely on particle range.

Disciplines

Engineering | Science and Technology Studies

Publication Details

Debrot, E., Newall, M., Guatelli, S., Petasecca, M., Matsufuji, N. & Rosenfeld, A. B. (2018). A silicon strip detector array for energy verification and quality assurance in heavy ion therapy. Medical Physics, 45 (2), 953-962.

Authors

Emily Debrot, Matthew Newall, Susanna Guatelli, Marco Petasecca, Naruhiro Matsufuji, and Anatoly B. Rosenfeld

A silicon strip detector array for energy verification and quality assurance in heavy ion therapy

Emily Debrot, Matthew Newall, Susanna Guatelli, and Marco Petasecca
Centre for Medical Radiation Physics, University of Wollongong, Wollongong, NSW 2500, Australia

Naruhiro Matsufuji
Research Centre for Charge Particle Therapy National Institute of Radiological Science, Chiba, Japan

Anatoly B. Rosenfeld[a)]
Centre for Medical Radiation Physics, University of Wollongong, Wollongong, NSW 2500, Australia

Purpose: The measurement of depth dose profiles for range and energy verification of heavy ion beams is an important aspect of quality assurance procedures for heavy ion therapy facilities. The steep dose gradients in the Bragg peak region of these profiles require the use of detectors with high spatial resolution. The aim of this work is to characterize a one dimensional monolithic silicon detector array called the "serial Dose Magnifying Glass" (sDMG) as an independent ion beam energy and range verification system used for quality assurance conducted for ion beams used in heavy ion therapy.

Methods: The sDMG detector consists of two linear arrays of 128 silicon sensitive volumes each with an effective size of $2\,\text{mm} \times 50\,\mu\text{m} \times 100\,\mu\text{m}$ fabricated on a p-type substrate at a pitch of 200 lm along a single axis of detection. The detector was characterized for beam energy and range verification by measuring the response of the detector when irradiated with a 290 MeV/u ^{12}C ion broad beam incident along the single axis of the detector embedded in a PMMA phantom. The energy of the ^{12}C ion beam incident on the detector and the residual energy of an ion beam incident on the phantom was determined from the measured Bragg peak position in the sDMG. Ad hoc Monte Carlo simulations of the experimental setup were also performed to give further insight into the detector response.

Results: The relative response profiles along the single axis measured with the sDMG detector were found to have good agreement between experiment and simulation with the position of the Bragg peak determined to fall within 0.2 mm or 1.1% of the range in the detector for the two cases. The energy of the beam incident on the detector was found to vary less than 1% between experiment and simulation. The beam energy incident on the phantom was determined to be (280.9 ± 0.8) MeV/u from the experimental and (280.9 ± 0.2) MeV/u from the simulated profiles. These values coincide with the expected energy of 281 MeV/u.

Conclusions: The sDMG detector response was studied experimentally and characterized using a Monte Carlo simulation. The sDMG detector was found to accurately determine the ^{12}C beam energy and is suited for fast energy and range verification quality assurance. It is proposed that the sDMG is also applicable for verification of treatment planning systems that rely on particle range.

Key words: energy verification, heavy ion therapy, Monte Carlo, QA, silicon strip detector

1. INTRODUCTION

Heavy ion therapy is a modality of growing interest in the field of radiotherapy[1] with several advantages over conventional photon beam treatments. These advantages are due to the physical energy deposition characteristics of charged particle beams as well as their increased biological effectiveness resulting from a high LET.

Heavy ions have a relatively small dose deposition in the entrance channel of the beam with the majority of the particle energy being deposited in the Bragg peak at the distal end of the particle range. Following this is a sharp dose fall off and a relatively small dose tail due to fragments. Heavy ions also exhibit little scattering thereby allowing a highly conformal dose delivery to be achieved in ion beam therapy. Therefore, is it possible to achieve tissue sparing of volumes proximal and distal to the target volume and the irradiation of cancerous
tissues located near sensitive structures.

The depth at which the Bragg peak occurs depends heavily on the medium being traversed, the heavy charged particle type and energy upon incidence. Hence, the dose delivered and its distribution within a patient due to heavy ion beams, used clinically in radiotherapy, is heavily dependent on the energy of the beam.

Due to the steep dose gradients associated with heavy ion beams, the Bragg peak must be delivered precisely within the target volume as deviations even in the order of millimetres within tissues can have severe implications, particularly in cases where the target volume is in close proximity to critical structures. As such it is crucial that the beam energy incident on the patient is precisely known; that is, quality assurance of the beam, in particular, range verification is of great importance for heavy ion therapy. Treatment planning systems implemented for heavy ion therapy are based on particle range using Monte Carlo methods and pencil beam approximations in heterogeneous materials (i.e., the patient).[2,3] Due to uncertainties in the ion beam range in heterogeneous materials like the patient anatomy, these treatment planning systems extend generous margins (typically _3 mm) to the prescribed target volumes. In order to reduce these margins and spare healthy tissues surrounding the target volume, particle range needs to be verified for TPS with submillimeter precision.

In order to verify beam characteristics for quality assurance in heavy ion therapy, a detector with high spatial resolution, that is capable of resolving steep dose gradients and suitable for beam entrance energy verification, is necessary. Historically, the gold standard for absolute dose dosimetry and beam verification is the ionization chamber. While these detectors are well characterized and are proven to have a high accuracy and reproducibility, they are expensive, are limited on the sensitive volume size and cannot provide the spatial resolution required.[4] Obtaining depth dose profiles using ionization chambers requires several measurements to be taken at varying depths in a phantom and is time intensive. Multilayer ionization chambers, such as the Magic Cube detector,[5] made up of strip-segmented ionization chambers separated by water equivalent blocks and the IBA Zebra dosimeter[6] have been developed for beam profiling and depth-dose measurements with reduced acquisition times. Such devices are still limited to a spatial resolution on the mm scale. Other detectors including radiographic and radiochromic films,[7–10] and diode dosimeters[11] have been investigated for relative depth dose and lateral profiling; all of which have their own limitations for ion range verification.[4]

The silicon strip serial Dose Magnifying Glass (sDMG) detector, developed at the Centre for Medical Radiation Physics (CMRP), University of Wollongong, is capable of measuring dose with sub-millimeter spatial resolution in MV photon therapy.12

The sDMG detector has been characterized using Monte Carlo simulations and experimental methods for application in proton therapy QA at beam energies corresponding to those used for ocular and prostate cancer therapy.13,14 The depth dose−response of a proton beam incident parallel to the axis of detection measured with the sDMG features two Bragg peaks, one due to the range of protons in the silicon detector and the second from protons scattered from the PMMA detector housing. It has been proposed that a range difference method be applied in order to determine the energy of the proton beam incident on the detector. This technique exploits the unique relationship between the energy of the proton beam at the entrance of the sDMG and the difference in the proton range measured between the two Bragg peaks. This paper presents both an experimental and Monte Carlo simulation based investigation of the sDMG detector in order to characterize the detector as a novel tool for verification of residual beam energy and ion range. The applicability of this detector for ^{12}C ion beam energy and range verification for QA procedures in heavy ion therapy facilities is investigated. A method to reconstruct the incident beam energy on the detector is presented and analyzed.

2. MATERIALS AND METHODS

2.A. sDMG Detector and data acquisition system

The Serial Dose Magnifying Glass, (Fig. 1, sDMG) is a multistrip silicon detector consisting of 256 channels formed from two linear arrays of sensors wire bonded end-to-end on a flexible printed circuit board (PCB). The linear arrays are each comprised of 128 n+ silicon strips implanted in a thin ptype silicon substrate. The diodes present a sensitive strip area of 0.05 9 2 mm2 with pitch 200 lm and measure along a single axis of length 50.8 mm. The total size of each silicon strip detector is 0.4 9 3 9 28 mm. The PCB is 0.5 mm thick and provides the fan-out for connection to the data acquisition system. The PCB and detector are contained within specifically recessed slabs of solid water providing suitable scattering conditions and mechanical rigidity.

Four TERA 64 channel chips were used to read out each of the 256 sensitive volumes of the sDMG detector. The TERA chip is an application specific integration circuit (ASIC) based on a current to frequency converter and digital counter. Each chip has a zero dead time readout with a high temporal resolution and large dynamic range. This DAQ system has been used in conjunction with previous generations of the sDMG detector and more information on the system specifics can be found in work by Wong12 and Fuduli.15

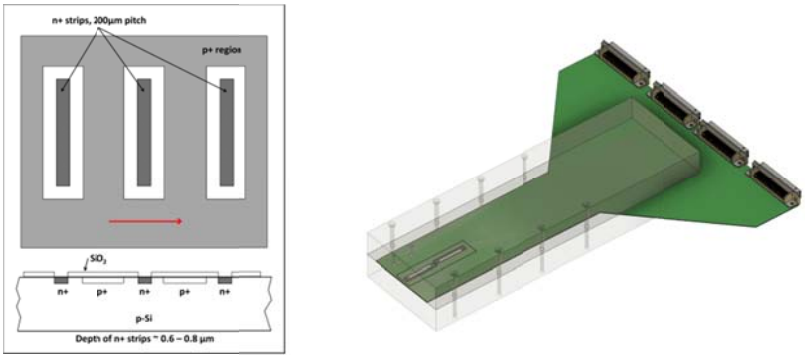

FIGURE 1. Schematics of the serial Dose Magnifying Glass (sDMG) comprised of two linear arrays detectors is wire bonded to a thin printed circuit board (PCB), the single axis of detection is indicated by the arrow.

2.B. Experimental setup

The results presented here are from experiments conducted at the Heavy Ion Medical Accelerator in Chiba (HIMAC), Japan. The beam line is shown schematically in Fig. 2 and consisted of an aluminum scattering filter, several meters of air, a brass collimator with a 10 × 10 cm^2 square opening (defining the field boundary) and PMMA phantom in which the sDMG detector was placed with the axis of detection aligned parallel to the incident beam direction. The sDMG is mounted on PCB and was surrounded by a small air recess within the PMMA phantom (see Figs. 1 and 3). The sensitive volumes of the detector were positioned in the center of the radiation field. Accurate alignment of the sDMG was achieved using laser beams and reference markers on top of the PMMA detector package which are aligned with the single axis of the sDMG detector. For the acquisitions the sDMG detector was operated in passive mode, with no external bias applied and was irradiated by a ^{12}C ion beam with an energy (E') of 290 MeV/u emerging from the vacuum head of the beamline.

The relative depth dose profiles of the beam were measured in the silicon detector with the front edge of the first detector at depths of 54, 89, and 102 mm in the PMMA phantom. The depth of the Bragg peak in silicon was determined from the position of the channel with the maximum response following equalization and was used to determine the beam energy incident on the detector (E_1) and the residual beam energy incident on the phantom (E_0).

(a) **(b)**

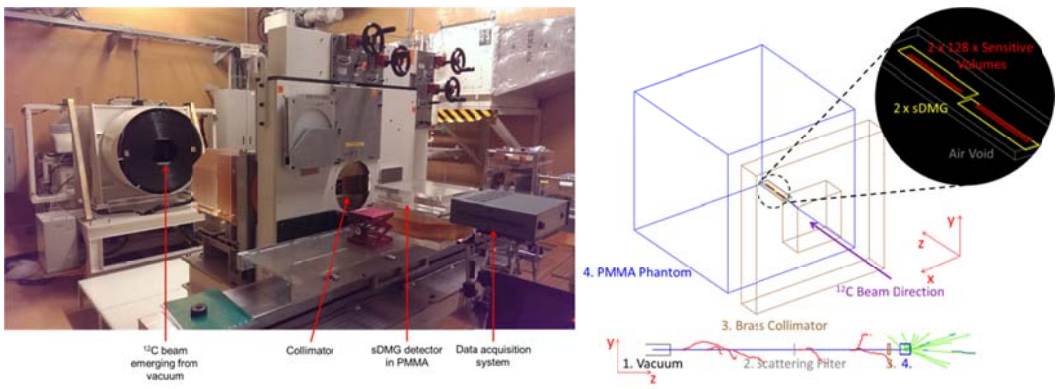

FIGURE 2. (a) sDMG detector embedded in PMMA phantom and with data acquisition system placed in experimental beamline, (b) schematic visualization of beamline from Geant4[16–18] simulation.

2.C. Uniformity/Equalisation

The response of the individual channels of the sDMG detector varies with the sensitivity and the corresponding preamplifier gain.19 This can result in variations in the response of detector channels. As such, a uniformity test was performed by exposing the detector to a uniform field and measuring the response of each individual channel (X_i). An equalization factor (F_i) was obtained for each channel and used to obtain an equalized channel response (X_{eq-i}) as given in Eq. 1, where X is the average response over all 256 channels. The detector response to a uniform field was obtained by orientating the detector face-on in a flat x-ray field produced by a 6 MV linac.

$$F_i = \frac{X_i}{\langle X \rangle} \rightarrow X_{eq-i} = \frac{X_i}{F_i} \tag{1}$$

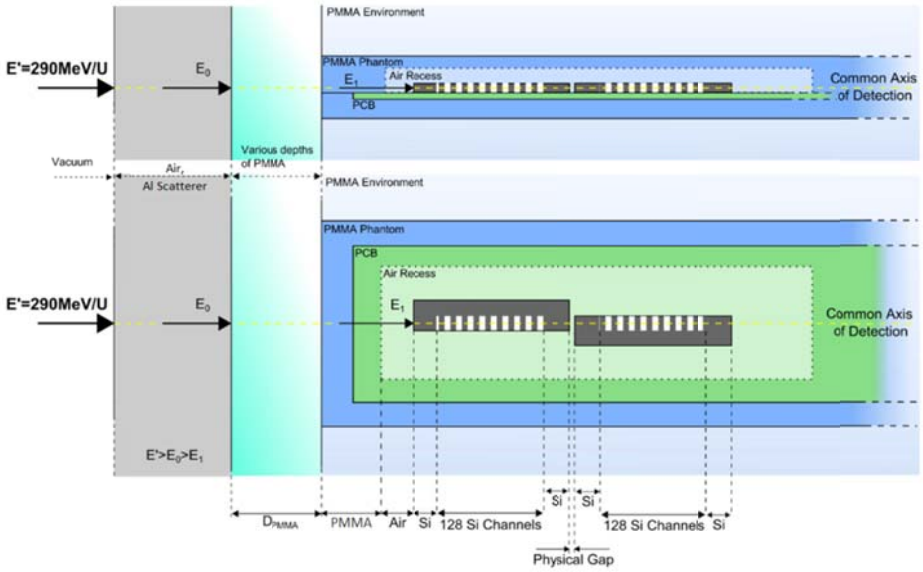

FIGURE 3. Detailed geometry of the sDMG in PMMA phantom for measurement of pristine Bragg peak (PBP) depth profile. The air void has an area 19 × 205 mm relative to the beams eye view; 6 mm of air is between the phantom wall and first silicon wafer of the detector and the physical gap between to two wafers is 0.6 mm.

2.D. Energy reconstruction method

The energy of the ion beam emerging from the vacuum (E') of the beam nozzle was 290 MeV/u in both experiment and simulation. The beam passes through several meters of air and a scattering filter resulting in a residual energy, E_0 at the face of the phantom. The energy of the beam incident on the detector after traversing the PMMA phantom, thickness *s*, is E_1. This is depicted in Fig. 3.

The energy of the beam incident on the detector E_1 was derived from the depth of the Bragg peak in the silicon detector and NIST data on the CSDA range20 in silicon as a function of particle energy.

$$R(E_0) = s + R(E_1) \tag{2}$$

The range of ions with residual energy E_0 incident on the PMMA phantom was calculated by noting the thickness of PMMA traversed s and $R(E_1)$, the range of the ions with energy E_1 in PMMA as given in Eq. 2, where R is the CSDA range for carbon ions of a given energy. The beam energy, E_0 incident on the PMMA phantom was then reconstructed from $R(E_0)$ again using the CSDA range data.

2.D. Geant4 simulation application

The experimental investigation of the sDMG response at the HIMAC facility in Japan was modeled using the Geant4 Monte Carlo Toolkit (version 10.1). As in the experimental setup the sDMG detector was placed with the common axis of detection parallel to the incident beam direction and in a PMMA phantom at depths of 54, 89 and 102 mm. The relative depth dose profile of the Bragg peak for a 290 MeV/u ^{12}C ion beam was calculated by scoring the total energy deposition in each of the 256 sensitive volumes of the sDMG detector.

The physics models set in the Geant4 simulation Physics List are shown in Table I. The alternative hadronic physics models Binary Ion Cascade Model (BIC), INCL++, QMD and QMD with *frag* option turned on, were compared in a first study. The results are shown in Section 3.A. The NIST material database was used to define the materials of the detector, phantom and beam line.

Particles were tracked from the point at which they emerge from the vacuum in the beam line. Beyond this point all elements of the experimental beam-line were modeled: over 6 m of air, an aluminum scattering filter and a brass collimator positioned before the PMMA phantom (see Fig. 2). The material *G4_PLEXIGLASS*, from the Geant4 NIST materials database, was used to define the PMMA phantom and the default density of 1.19 g/cm^3 was used. This material coincides with that used in the experimental setup and the NIST range data used to reconstruct the beam energy incident on the phantom. With the exception of the PCB board, that was excluded due to uncertainty in its material composition, the detector construction was consistent with the experimental setup.

Physics Processes	Geant4 Models
Electromagnetic physics	G4EmStandardPhysics_option3
Decay physics	G4DecayPhysics
Radioactive decay physics	G4RadioactiveDecayPhysics
Hadronic physics	G4HadronicPhysicsQGSP_BIC_HP G4HadronElasticPhysicsHP G4StoppingPhysics G4EmExtraPhysics Hadronic Ion Physics Model (BIC, INCL++, QMD and QMD with frag option on)

TABLE 1.Geant4 Physics models used in the simulation Physics List

The internal potential difference established between each n^+ electrode and the p-type silicon substrate of the detector results in a depletion region around the electrode. The size of this depletion region represents the sensitive volume of each diode in the sDMG array. The effective size of the sensitive volumes was determined using an ion beam induced charge (IBIC) collection study technique based on scanning the unbiased detector with a 1 μm diameter 8 MeV proton or 5.5 MeV 4He ion beam. These studies revealed laterally diffused charge collection within 50 μm of the electrode. The size of the scoring volumes defined for the simulation were adjusted to replicate this charge collection region - the depth of each sensitive volume was defined to be 50 μm and the width 100 μm (accounting for diffused charge from either side of the electrode). While this diffusion region affects the size of each sensitive volume it does not directly reflect the spatial resolution of the sDMG since the position of each n^+ contact is well-defined. The dimensions of the contacts and sensitive volume size used in the simulation are given in Table II.

A total of 3×10^7 primaries were tracked for each simulation with their starting position randomly generated on the downstream face of the vacuum window within an area of 5×5 cm^2 centered on the beam axis. The initial kinetic

energy of each primary was 290 MeV/u. No angular or energy dispersion was modeled in the generation of primary ions as each ion undergoes multiple scattering events over its trajectory in the beam-line thus providing some variation in the angular dispersion of primaries incident on the phantom and detector. Furthermore, this multiple scattering, particularly when particles traverse the scattering filter, results in an increasing field size with distance along the beam-line. The field size at the point of primary generation was reduced for the simulation component of this study in order to optimize the simulation and increase statistics for the interaction of particles within the detector. Prior to this an investigation on the effects of the generated field size on the depth of the Bragg peak in the silicon detector was performed and showed no field size dependence on the relative peak position. The results of this investigation are presented in Section 3.A. The simulation was further optimized in terms of execution times by appropriately using the *Geant4 Cuts Per Region*. The simulation was also used to investigate the effect of the air gap surrounding the sDMG detector on its response as well as to characterize the potential advantages of the proposed next generation of single axis silicon strip detector. The findings are presented in Section 3.C.

	sDMG	Simulated sDMG collection regions
Channels	256	256
Pitch	200 μm	200 μm
Strip area	$20 \times 2000\ \mu m^2$	$100 \times 2000\ \mu m^2$
Strip depth	$0.6 - 0.8$ μm	50 μm

TABLE 2. sDMG Dimensions.

3. RESULTS AND DISCUSSION

3.A. Geant4 simulation optimization: investigating detector response for alternate hadronic physics models and variable field size

Figure 4(a) shows the simulated profiles obtained using the hadronic ion physics models INCL++, BIC, QMD, and QMD with the *frag* option turned on for the detector at a depth of 54 mm in the PMMA phantom. The primary difference between the models is seen in the fragmentation tail distal to the Bragg peak as the species and yield of the fragments produced are dictated by the hadronic physics model used. Given the similar energy deposition profiles with alternate Geant4 fragmentation models, the INCL++ model was chosen as it was found to have a quicker execution time.

(a)

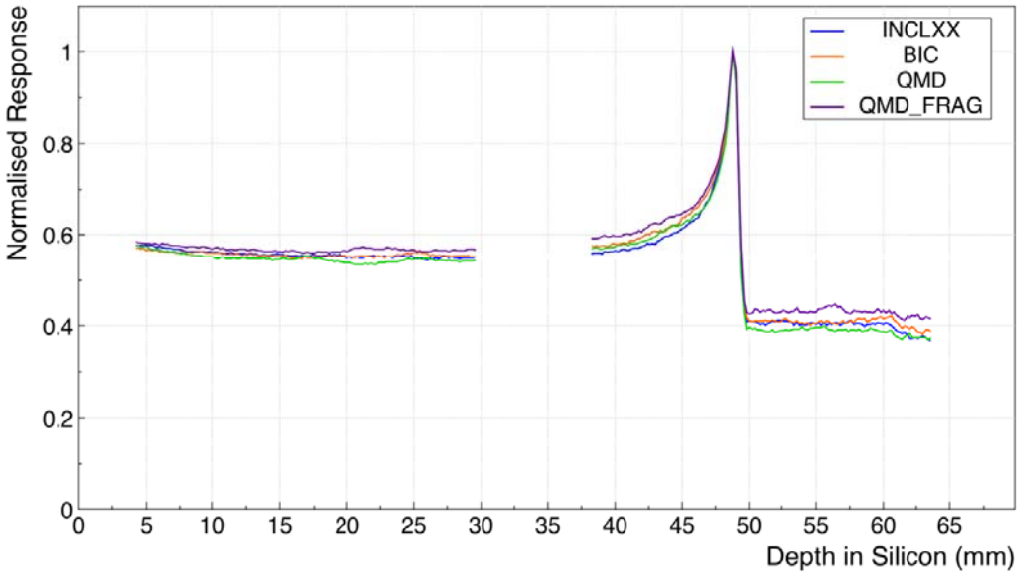

(b)

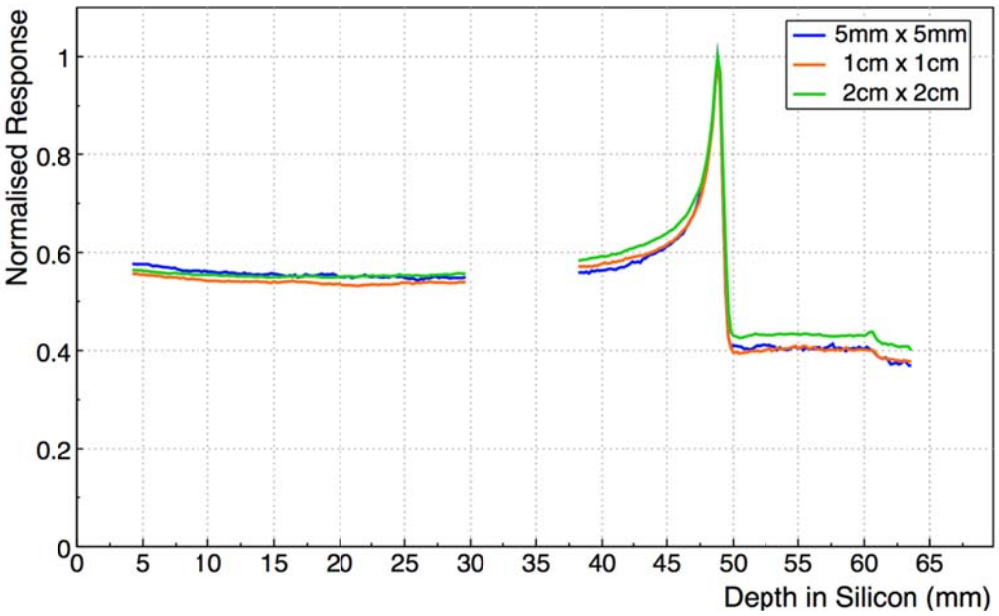

FIGURE 4.Comparison of resulting pristine Bragg peak calculated in the sDMG detector for (a) alternate Geant4 ion hadronic physics models and (b) different generated field sizes. The sDMG is set at a depth of 54 mm in PMMA. The discontinuity in the center of the plot (and in Figs. 5–9) is due to the physical separation in sensitive volumes between the end of the first and the start of the second silicon strip detectors comprising the sDMG [see Figs. 1 and 2(b)]. Profiles are normalized to the pixel with the maximum energy deposition.

The effect of varying the initial field size of the beam on the sDMG response is depicted in Fig. 4(b). Here, the particle flux was held constant for the three field sizes shown. The relative energy deposition in the buildup to and downstream of the Bragg peak is seen to increase slightly with the field size. This variation in the relative profile shape is attributed to increased scatter contribution of primaries and fragment ions scattering from the surrounding

phantom into the detector. With greater generated field sizes a secondary Bragg peak (discussed in Section 3.C) still cannot be clearly resolved. Furthermore, the application of the sDMG detector for ^{12}C ion range measurement and energy reconstruction relies only on the depth of the Bragg peak in the silicon detector to be accurately determined and does not concern the shape of the profile. As such, the field size was reduced to 5×5 mm^2 in order to increase statistics in the sensitive volumes of the detector whilst reducing computational time.

The relatively high energy deposition beyond the Bragg peak is due ions traversing the surrounding PMMA and scattering into the detector; this effect is further discussed in Section 3.C.

3.B. Comparison of experimental and simulation results

The pristine Bragg peak profiles measured in the silicon detector with different thicknesses of PMMA phantom placed in front are shown in Figs. 5–7. The measured positions of the Bragg peak in silicon, the reconstructed energy, E_1, of the beam incident upon the detector and the residual energy, E_0, of the beam incident on the phantom are shown in Table III. The range of ^{12}C ions in silicon, which is indicated by the position of the Bragg peak, is shown to have excellent agreement between experiment and simulation with no more than 0.2 mm difference in the position. While there is strong agreement in the peak positions, several differences arise in the shape of the experimental and simulated dose profiles in silicon. These differences are largely attributed to the non-linear variations in the response of individual sensitive volumes to ^{12}C ions due to their variable LET and to radiation damage (defects) along the sDMG detector while the applied equalization factor was based on the response of the detector in a 6 MV x ray field from a linac with uniform, low LET from Compton electrons. The local peaks observed at depths of approximately 13, 21 and 27 mm in silicon for the experimental profiles are an example of this where defects were induced from previous irradiations with varying entrance energies and Bragg peaks at these depths.

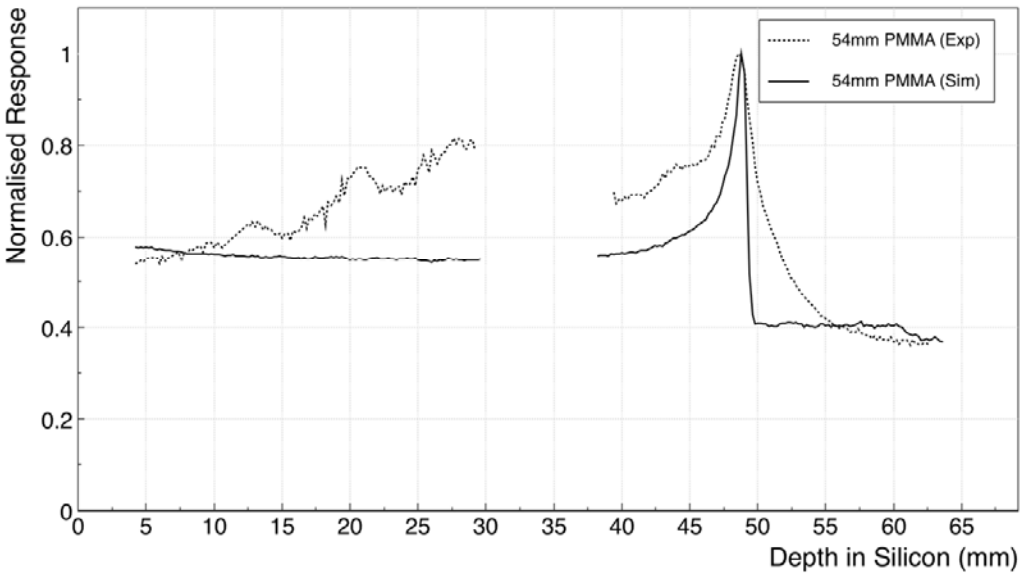

FIGURE 5. Resulting pristine Bragg peak measured experimentally with the sDMG detector and calculated in the Geant4 simulation at a depth of 54 mm in PMMA.

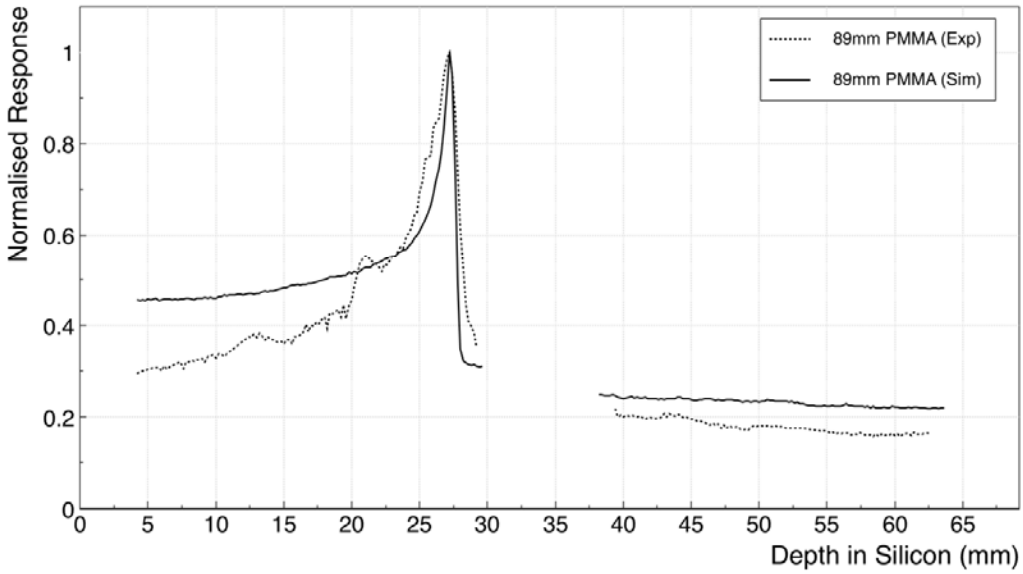

FIGURE 6. Resulting pristine Bragg peak measured experimentally with the sDMG detector and calculated in the Geant4 simulation at a depth of 89 mm in PMMA.

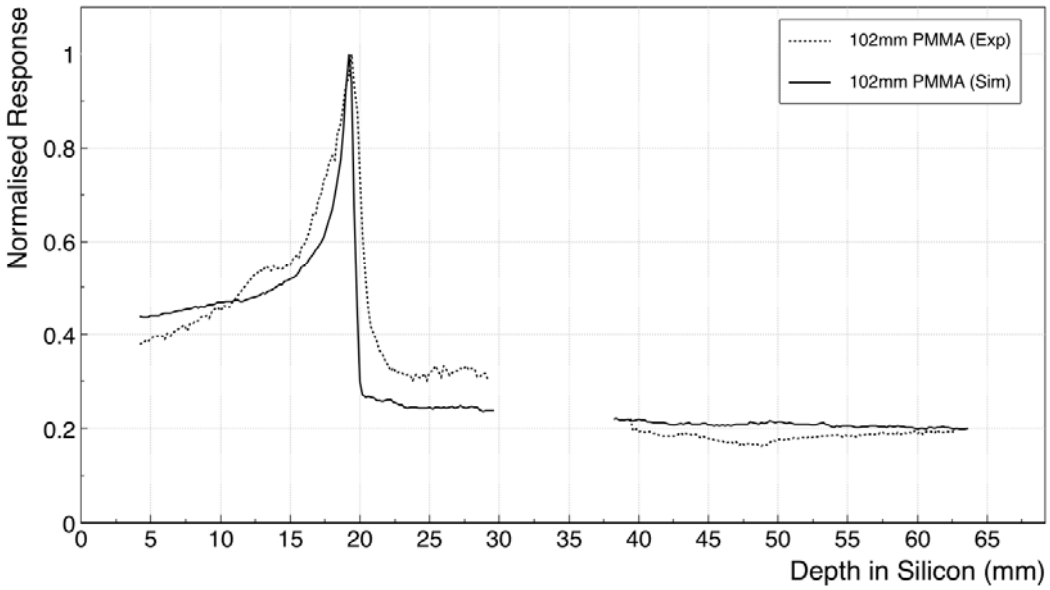

FIGURE 7. Resulting pristine Bragg peak measured experimentally with the sDMG detector and calculated in the Geant4 simulation at a depth of 102 mm in PMMA.

The detector response for the experimental profiles with 89 and 102 mm of PMMA placed at the entrance of the sDMG (Figs. 6 and 7, respectively) are seen to lack the typical "flat" plateau region proximal to the buildup to the Bragg peak. The increasing detector signal with depth in the silicon detector highlights the non-linear response of the silicon sensitive volumes to changes in particle LET. The simulation presents the ideal case where the charge

collection efficiency in pixels is 100% and cross-talk or charge sharing between sensitive volumes as well as LET dependent recombination of charge carriers does not occur.

The distal falloff of the experimental Bragg peak profiles are not as sharp as the simulated profiles. This is because the PCB board is not modelled in the simulation. Since the stopping power of ^{12}C ions in PCB is less than in silicon, ions that travel through the PCB and undergo lateral scattering into the silicon detector will have a range exceeding that of ions travelling in silicon only. The result is energy deposition beyond the Bragg peak and a broadening of the distal falloff, particularly in Fig. 5 where the particle range in the detector (and potentially in the PCB) is greatest.

The average residual energy of the beam incident on the phantom, E0, was calculated for experiment and simulation to be (280 $\pm$ 0.8) MeV/u and (280 $\pm$ 0.2) MeV/u, respectively (uncertainty stated to 2σ); these values agree within experimental error. The 290 MeV/u beam traverses an aluminium scatterer and several meters of air before incidence on the phantom. The energy of the beam entering the phantom was estimated to be approximately 281 MeV/u by considering the combined water equivalent thicknesses of the scattering material and air and the range in water of the ions emerging from the vacuum of the beam head (again employing the method using Eq. 2). A Geant4 simulation calculating the energy of the beam at the end of the beamline used in the experiment also revealed an average particle energy of 282 MeV/u.

3.C. Optimization of the DMG design: Simulation study of the effect of air gaps in the DMG response

The dependence of the detector response on the size of the air gap surrounding the detector inside its PMMA casing was investigated using the Geant4 application discussed previously by varying the height of the air gap above the plane of the silicon sDMG. The physics list used for the simulation here is the same as in Table I. The actual height of the air void was measured to be 2.5 mm and this value was used in the profiles simulated in Figs. 5–7. Figure 8 shows the profiles obtained with the sDMG placed at a depth of 54 mm in the phantom for an air void 0.5, 1, and 2.5 mm in height.

An obvious increase in energy deposited downstream of the Bragg peak is observed for a 0.5 mm air gap only. Energy deposition beyond the Bragg peak is attributed to carbon ions and fragments scattering from the surrounding phantom into the detector as particles traversing the phantom have a greater range than those travelling through the silicon detector due to the greater stopping power of the latter. As high energy carbon ion beams primarily undergo small angle Coulomb scattering they are likely to traverse the airgap without entering the sDMG for the cases with a 1 and 2.5 mm airgap. Particles that traverse the phantom and scatter into the detector contribute to a secondary Bragg peak in the detector beyond that produced by carbon ions in silicon provided the detector is long enough to accommodate both Bragg peaks.

The position of this secondary Bragg peak corresponds to the particle range in the PMMA phantom. The secondary Bragg peak is not observed in Fig. 8 as the range of the ^{12}C ions in PMMA is beyond the length of the sDMG placed at this depth. Figure 9 shows the effect of changing the size of the air gap on sDMG response with the sDMG entrance placed at a depth of 102 mm in the phantom. This plot shows the detector response for two air void sizes for both the sDMG design described previously and for the proposed next generation single monolithic DMG that will be approximately 60 mm long with 256 sensitive volumes. It should be noted that the dose deposition profiles in

silicon for the sDMG and the next generation single monolithic DMG are near identical for the same size surrounding air void only the response of the new DMG design allows a continuous profile to be observed compared to the gap associated with the spacing between the sensitive volumes of the two wafers in the sDMG design. The simulated secondary Bragg peak is clearly observed for the 0.5 mm airgap. This secondary Bragg peak however has no distinct falloff and lies beyond the expected range of the primary ^{12}C ions in PMMA (indicated by the red line). Ions contributing to this peak will have traversed the small air gap between the phantom and the detector and (due to the comparatively low stopping power of the air) their range will be perpetuated further.

Figure 9 also presents the response of the new DMG detector design for an optimum setup with no air gap between the phantom and silicon of the detector. For this case, the falloff of the secondary Bragg peak can be clearly seen and is aligned (at approximately the 60% falloff mark) with the expected range of the ^{12}C ions in the PMMA phantom only. With this optimized design of the DMG detector a second method of range verification becomes possible where the range of an ion beam in the phantom is determined from the absolute position of the secondary Bragg peak measured in the detector. Due to these findings, future DMG designs will adopt the single wafer design and endeavor to be closely fitted with a PMMA sheath/carrier in order to increase scatter conditions and thus detector response.

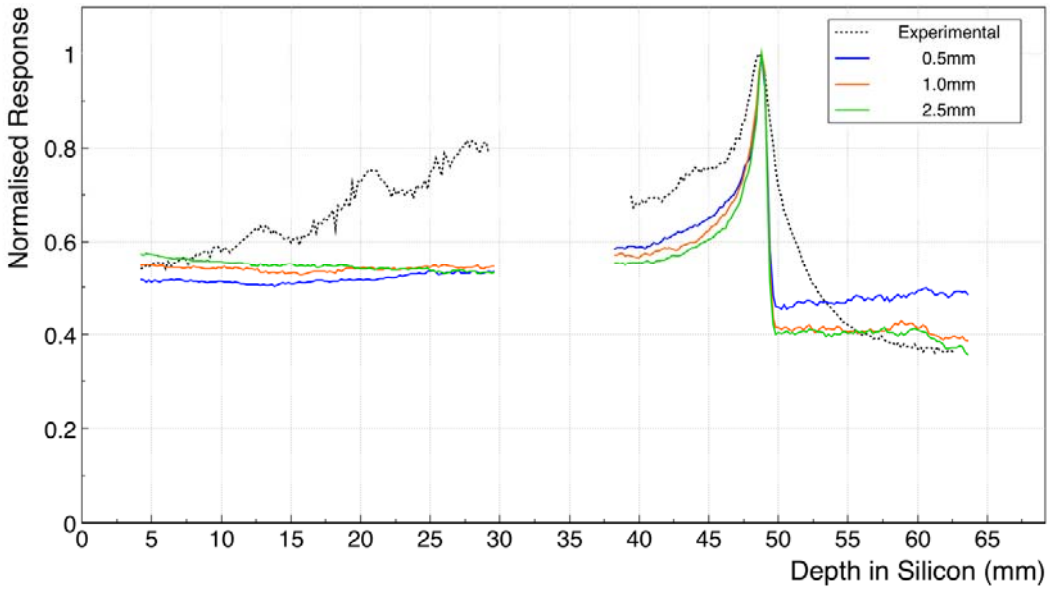

FIGURE 8. Calculated pristine Bragg peak in the sDMG with a surrounding aid void with heights of 0.5, 1.0 and 1.5 mm using the Geant4 simulation and the detector places at 54 mm in PMMA.

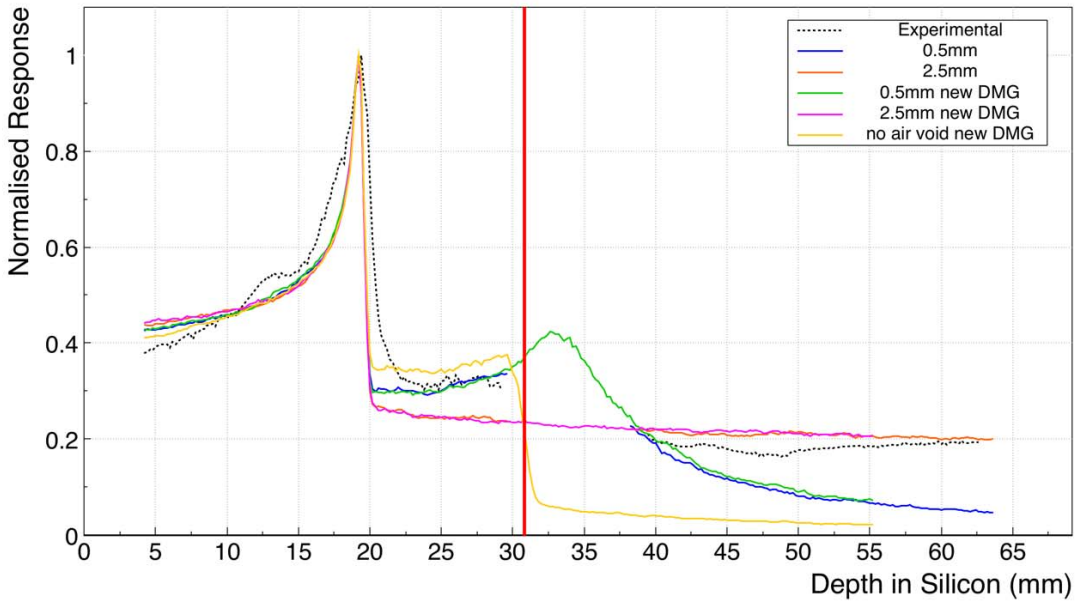

FIGURE 9. Calculated pristine Bragg peak in sDMG detector and new proposed single wafer DMG for air void heights of 0.5 and 2.5 mm and without an air void, at a depth of 102 mm in PMMA. The vertical line indicates the expected range of carbon ions in PMMA relative to the detector position.

In summary, two modes of QA operation are possible for the current device and method: (a) verification of ^{12}C ion beam energy after traversal of homogeneous or heterogeneous media and (b) energy reconstruction of ions incident on a PMMA phantom of known density and thickness (or other known homogeneous material) in front of sDMG. The simulation component of the study indicates that the future DMG design may be used to directly measure the absolute range of an ion beam in a homogeneous or heterogeneous phantom from the secondary Bragg peak observed.

Moreover, the sDMG is proposed as a tool for validation of treatment planning systems or Monte Carlo simulations by reconstructing the energy loss of ions in materials upstream of the sDMG and, for future generations of the detector, using direct measurement of the particle range.

While in most silicon diodes the response is effected by the LET of charged particles, the proposed sDMG or single monolithic DMG do not require accurate measurement of absolute dose for depth profiles in silicon, rather precise measurement of the Bragg peak position is sufficient for range and beam energy reconstruction. The same is true for radiation damage in the detector that can change the relative depth dose–response whilst leaving the Bragg peak position unaffected.

4. CONCLUSIONS

The Serial Dose Magnifying Glass (sDMG) is a multistrip detector designed for high spatial resolution dose profiling in silicon and subsecond temporal resolution. The detector consists of two linear arrays of 128 n+ silicon strip diodes fabricated on a p-type silicon substrate with a single axis of detection. Each strip diode has an effective sensitive volume of approximately $2\ \text{mm} \times 50\ \mu\text{m} \times 100\ \mu\text{m}$ at a pitch of 200 μm.

This study demonstrates that the sDMG detector is a fast and powerful independent QA tool for therapeutic ^{12}C ion beams. The sDMG was characterized for energy verification by measurement of the Bragg peak profiles for a 290

MeV/u ^{12}C ion beam with the silicon detector embedded at various depths in a PMMA phantom. The depths of the Bragg peak in the silicon detector measured experimentally at the HIMAC facility and using Monte Carlo simulations were found to fall within 0.2 mm for the two methods and consequently the calculated energy of the beam incident on the detector was found to agree within experimental error. The reconstructed residual energy of the beam incident on the PMMA phantom was determined to be (280.8 ± 0.8) MeV/ u from the experiment and (280.8 ± 0.8) MeV/u from the simulation. The energy of the beam incident on the phantom was found to agree with the expected energy.

ACKNOWLEDGMENTS

We thank the University of Wollongong Information Technology Services (ITS) for computing time on the UOW High Performance Computing Cluster. This research is supported by an Australian Government Research Training Program (RTP) Scholarship. This research is partially supported by Australian Research Council Grant DP 170102273.

REFERENCES

1. Jäkel O, Schulz-Ertner D, Karger C, Nikoghosyan A, Debus J. Heavy ion therapy: status and perspectives. *Technol Cancer Res Treat.* 2003;2:377–387.
2. Inaniwa T, Furukawa T, Kanai T, et al. Development of treatment planning for scanning irradiation at HIMAC. *Nucl Inst Methods Phys Res B.* 2008;266:2194–2198.
3. Krämer M, Jäkel O, Haberer T, Kraft G, Schardt D, Weber U. Treatment planning for heavy-ion radiotherapy: physical beam model and dose optimization. *Phys Med Biol*. 2000;45:3299–3317.
4. Christian PK, Oliver J, Hugo P, Tatsuaki K. Dosimetry for ion beam radiotherapy. *Phys Med Biol*. 2010;55:R193–R234.
5. Cirio R, Garelli E, Trevisiol E, et al. Two-dimensional and quasi-threedimensional dosimetry of hadron and photon beams with the Magic Cube and the Pixel Ionization Chamber. *Phys Med Biol*. 2004;49:3713–3724.
6. Dhanesar S, Sahoo N, Gillin M, et al. Quality assurance of proton beams using a multilayer ionization chamber system. *Med Phys.* 2013;40:092102.
7. Heeg P, Hartmann G, Jäkel O, Karger C, Kraft G. Quality assurance at the heavy-ion therapy facility at GSI. *Strahlenther Onkol*. 1999;175:36–38.
8. Hara Y, Furukawa T, Mizushima K, Takeshita E, Shirai T, Noda K. Application of radiochromic film for quality assurance in the heavy-ion beam scanning irradiation system at HIMAC. *Nucl Inst Methods Phys Res B.* 2014;331:253–256.
9. Spielberger B, Krämer M, Kraft G. Three-dimensional dose verification with x-ray films in conformal carbon ion therapy. *Phys Med Biol*. 2003;48:497–505.
10. Spielberger B, Scholz M, Krämer M, Kraft G. Experimental investigations of the response of films to heavy-ion irradiation. Phys Med Biol. 2001;46:2889–2897.
11. Kaiser F, Bassler N, Jäkel O. COTS Silicon diodes as radiation detectors in proton and heavy charged particle radiotherapy 1. *Radiat Environ Biophys*. 2010;49:365–371.
12. Wong J, Carolan M, Rosenfeld A, et al. A silicon strip detector dose magnifying glass for IMRT dosimetry. *Med Phys*. 2010;37:427–439.

13. Merchant A, Newall M, Rosenfeld A, et al. Feasibility study of a novel multi-strip silicon detector for use in proton therapy range verification quality assurance. *Radiat Meas*. 2017;106:378–384.
14. Merchant A, Guatelli S, Petesecca M, Jackson M, Rozenfeld A. Monte Carlo characterisation of the Dose Magnifying Glass for proton therapy quality assurance. *J Phys*. 2017;777:1
15. Fuduli I, Newall M, Petasecca M, et al. Multichannel Data Acquisition System comparison for Quality Assurance in external beam radiation therapy. *Radiat Meas*. 2014;71:338–341.
16. Agostinelli S, Allison J, Cooperman G, et al. Geant4-a simulation toolkit. *Nucl Instrum Methods Phys Res, Sect A*. 2003;506:250.
17. Allison J, Amako K, Apostolakis J, et al. Geant4 developments and applications. *IEEE Trans Nucl Sci*. 2006;53:270–278.
18. Allison J, Amako K, Yoshida H, et al. Recent Developments in Geant4. *Nucl Inst Methods Phys Res A*. 2016;835:186–225.
19. Aldosari A, Petasecca M, Rosenfeld A, et al. A two dimensional silicon detectors array for quality assurance in stereotactic radiotherapy: Magic- Plate-512. *Med Phys*. 2014;41:091707.
20. Linstrom PJ, Mallard WG, Eds., *NIST Chemistry WebBook, NIST Standard Reference Database Number 69*, Gaithersburg MD: National Institute of Standards and Technology, 20899, http://webbook.nist.gov